Chem. Senses 29: 235–245, 2004 DOI: 10.1093/chemse/bjh028

Modeling the Kinetics of Flavour Release during Drinking

Valéry Normand, Shane Avison and Alan Parker

Firmenich S.A., 7 rue de la Bergère, 1217 Meyrin 2 Geneva, Switzerland

Correspondence to be sent to: Dr Valéry Normand, Firmenich S.A., 7 rue de la Bergère, 1217 Meyrin 2 Geneva, Switzerland. e-mail: valery.normand@firmenich.com

Abstract

Novel mathematical models for flavour release during drinking are described, based on the physiology of breathing and swallowing. Surprisingly, we conclude that most flavour molecules arriving in the nose are extracted from liquid left in the throat, after swallowing. The models are fit to real time flavour release data obtained using APCI–mass spectrometry. Before modelling, raw data are corrected for the effects of varying airflow rate, using the signal from acetone in exhaled air. A simple equilibrium batch extraction model correctly describes flavour release during the first breaths after swallowing a flavoured liquid. It shows that for eight volatiles, whose *in vitro* air–water partition coefficients vary by a factor of 500, the apparent *in vivo* air–saliva partition coefficients vary only by a factor of five. To interpret the kinetics of flavour release longer after swallowing, diffusion of flavour into the throat lining is included. This is done using a three-layer model for mass transfer in the throat. An analytical solution of this model gives good fits to typical data. These models de-couple the physiological and physico-chemical aspects of flavour release, clarifying the effect of behaviour on *in-vivo* flavour release.

Keywords: flavour release, mass-transfer, physiology

Introduction

The goal of cognitive science is to understand how perception is related to sensory stimuli. For the olfactive component of flavour (the aroma of food during eating) this approach was impossible until recently because the stimulus, the concentration of flavour molecules on the nasal epithelium, was unknown. The situation has changed now that the concentration of flavour molecules in air exhaled through the nose can be measured in real time, using mass spectrometry (a recent review is Taylor and Linforth, 2000).

The aim of this study is to better understand the physiological and physico-chemical origins of the variation in the kinetics of flavour release. We are particularly interested in the influence of food composition (fat content, for instance). Improved modelling should improve our understanding of how flavour composition, anatomy and physiology influence flavour release.

Existing mathematical models for *in vivo* (or 'in mouth') flavour release are adaptations of models for *in vitro* release (for a review, see Taylor, 2002). However until now they have not correctly incorporated the physiology of eating and drinking. Invariably, flavour-rich air in the mouth is assumed to pass directly into the nose (e.g. Harrison, 1998, 2000). This assumption is almost always incorrect, as there is a gas-tight seal between mouth and nose for most of the time (Buettner *et al.*, 2001). During eating this seal is not perfect, so flavour can reach the nose intermittently during chewing. During drinking, which we study here, the seal is perfect, except when swallowing.

The paper is structured as follows. First we describe the physiology of swallowing. Then we discuss the raw data from flavour release and describe some essential improvements to the data treatment. Finally, we describe two different mathematical models for flavour release, comparing each with experimental data to show its strengths and weaknesses.

Physiology of swallowing

The throat is used for both breathing and feeding, so each swallow involves a risk. This is especially true during drinking, as even a small opening at the back of the mouth will allow liquid food to flow into the lungs, with a risk of infection or choking. Recent studies of the physiology of swallowing (Dodds *et al.*, 1990a,b; Firmin *et al.*, 1997) aim to better understand potentially fatal malfunction of the swallowing reflex. They also help to better understand flavour release. Figure 1 shows the anatomy of the upper digestive tract schematically, approximated by a series of tubes and cavities. It is centred around a single tube, a portion of the pharynx between the back of the tongue and the entrances to the larynx and the oesophagus.

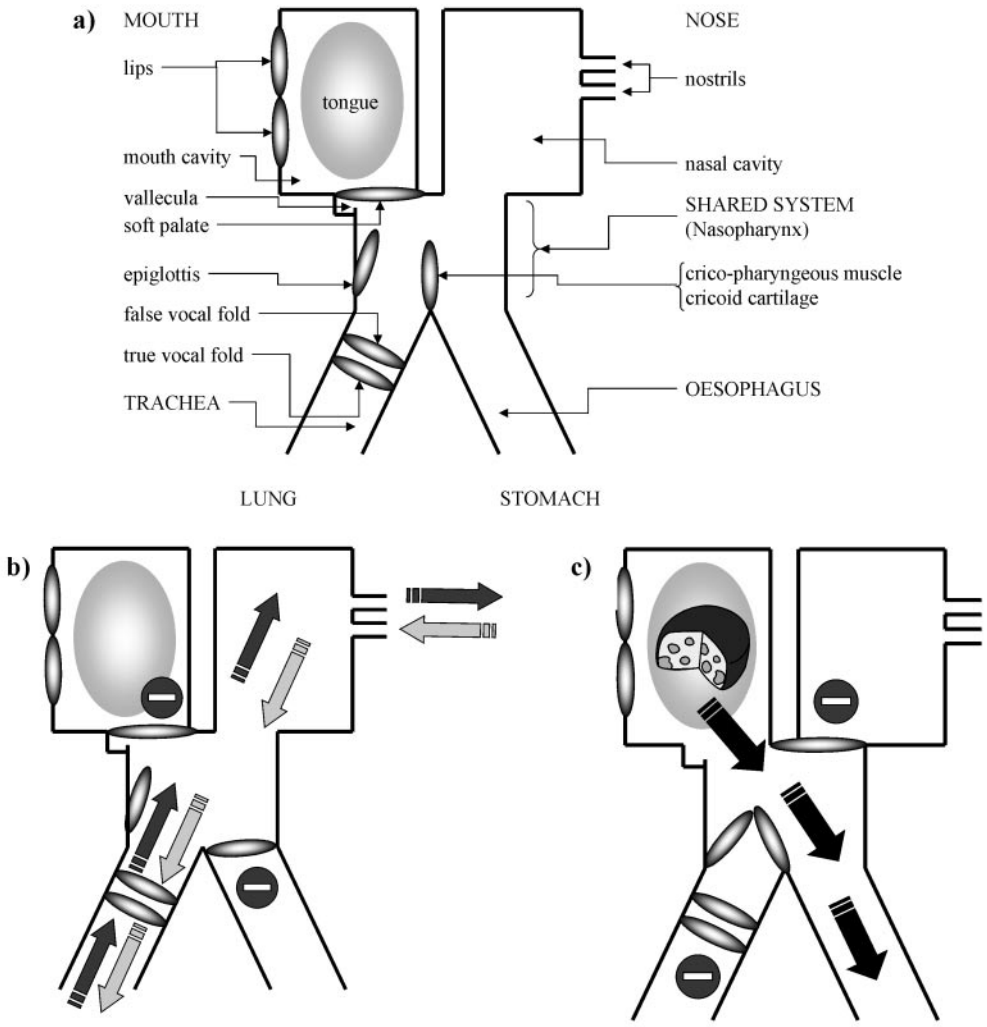

Figure 1 **(a)** Schematic anatomy of the feeding and breathing systems. **(b)** Configuration during breathing. **(c)** Configuration during swallowing.

At the upper end this tube separates to form two cavities: the mouth for feeding and the nasal cavity for breathing. At the lower end the tube also divides into two: the oesophagus, for feeding, and the trachea, for breathing. The mechanisms represented in Figure 1b,c are well described elsewhere (Bosma, 1980), from which the following key points arise: This system of valves almost completely prevents flavour molecules released from liquid food in the mouth from reaching the nose. The only exception is the 'swallow breath' immediately after swallowing (Land, 1994). The flavour release mechanism concerns throat and nasal cavities only. Flavour entering the oesophagus is lost for retronasal release.

Materials and methods

Flavour release in expired air was measured using atmospheric pressure chemical ionization–mass spectrometry (APCI–MS; Micromass, Manchester, UK) (Taylor *et al.*, 2000). A patented interface (Linforth and Taylor, 1998) diverts a fraction of the expired air into the mass spectrometer. This technique of sampling exhaled air has been called 'nose space', by analogy with the headspace technique for sampling air samples *in vitro*. Samples of the breath were drawn at 35 ml/min into the ionization source through a heated (160°C) deactivated fused silica tubing to prevent condensation of the volatile compounds. Compounds entering the source were ionised by a 4 kV positive ion corona pin discharge and the ions formed were introduced into the high vacuum region of the mass spectrometer, where they were separated and detected according to their m/z ratio as described previously (Taylor *et al.*, 2000). The volatiles studied were detected at masses corresponding to their protonated molecular ion (MH^+). Absolute measurement of flavour intensity is still under consideration regarding the chemical ionization process and transfer of the ions to the mass spectrometer. However, all other things being equal, in this study, relative rather than absolute values are taken to characterize the kinetics of the flavour release. The selectivity and the sensitivity of the mass spectrometer are constant over the duration of one experiment.

Panellists were asked to swallow according to the following protocols.

- Protocol 1: freely.
- Protocol 2: (i) hold mouth shut without swallowing for 2 min; (ii) inject 8 ml of flavoured solution into closed mouth; (iii) hold solution in mouth for 30s; (iv) swallow all the solution; and (v) breath normally through the nose, keeping mouth shut. The subjects were given no other instructions on how to breathe.
- Protocol 3: identical to protocol 2 except that the subjects were asked to breathe at a given frequency.

Volatiles in the exhaled breath were recorded using the nose space technique for several minutes. The flow rate of inhaled and exhaled air was recorded in real time using a physiological air flow meter (World Precision Instruments, Stevenage, UK). It was placed in-line with the APCI–MS interface, so that the flow rate and composition of expired air were measured simultaneously.

Results

Effect of behaviour on the kinetics of flavour release

Real time measurements show that the kinetics of flavour release is extremely subject-dependent. This point is illustrated in Figure 2, which shows the flavour concentration in exhaled air for three subjects drinking the same menthol solution with no artificial restrictions on their behaviour (protocol 1).

These patterns of flavour release show huge differences, due to the different ways in which people breathe and swallow. It is very likely that the perceptions resulting from these different stimuli will also be different. Electromyography measurements are needed to directly determine the panellist's behaviour whilst measuring flavour release (Hodgson *et al.*, 2003). As we could not do this, we can only emphasize the fact that behaviour greatly influences the flavour release profile. For the rest of the work discussed here, we imposed a protocol to avoid the effects caused by multiple swallowing. The question then is: what is the origin of the sequences of flavour peaks in Figure 2? Our answer, in line with the physiology, is that they must be due to flavour extracted by exhaled air from residual liquid coating the throat after swallowing. This explanation is the key point that we want to make. The idea that flavour extraction from the throat lining is a major part of the signal in the nose is original. Buettner *et al.* (2002) discuss the idea briefly, but do not emphasize it. The recent review by Taylor (2002) does not mention this idea.

In fact, Land speculated 10 years ago (Land, 1994) that the only source of aroma compounds in the nose during eating was from the small 'swallow breath' immediately after swallowing. Buettner *et al.* (2001) agreed with this point of view, on the basis of their study using videofluoroscopy and real-time MRI. Figure 2 shows that this is not the case. Significant amounts of aroma compound are exhaled from the nose in every breath, even 1 min after swallowing.

Improved data treatment

A major problem in interpreting raw nose-space data is that the signal is proportional to the amount of flavour per unit time, which is the product of the air flow rate and the flavour concentration. Breathing faster will have exactly the same effect on the signal as increasing the flavour concentration, so an unusually large peak could be due to either higher flavour concentration or faster exhalation. Unambiguous interpretation of the raw data is impossible. The simplest way to remove this ambiguity is to measure the air flow rate in the nose. However, physiological air flow meters are expensive and integration of the flow rate and flavour release data is tedious. A more practical solution would be to use an internal standard. The internal standard should be easy to measure in the exhaled air and its concentration must not change during an experiment. We find that acetone is suitable. It is produced by fat metabolism in the liver and then passes into the blood. It partitions from the blood stream into the lungs and so is present in exhaled air. It is easily measured by the nose-space technique.

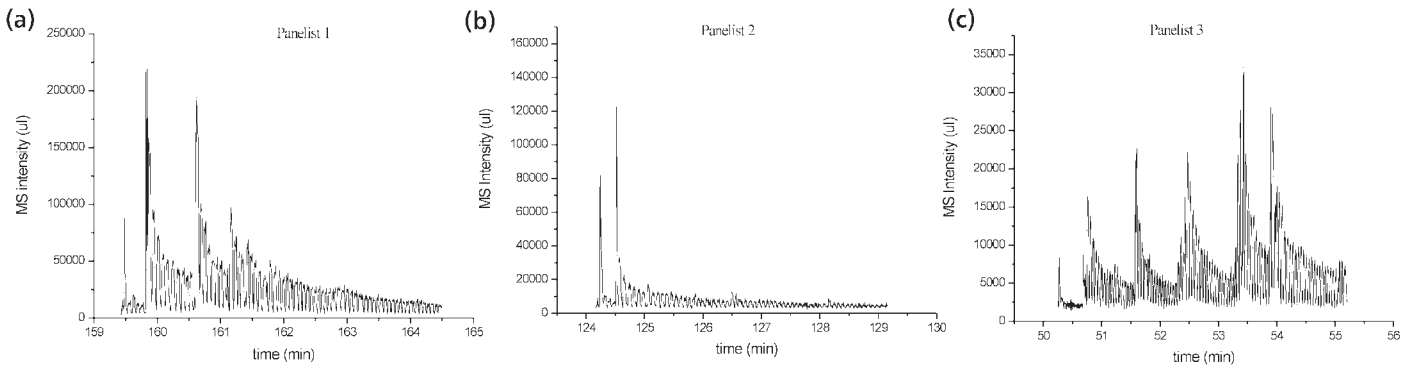

Figure 2 Flavour release from menthol solution consumed by three different subjects. Each large peak corresponds to a swallow. Panellist 3 is a flavourist, who makes many small swallows. This behaviour clearly prolongs the flavour release.

We made a series of measurements of acetone peak area and exhaled volume per breath. The measurements used one subject and lasted >1 h. Plotting peak area against breath volume gave a good straight line (r^2 = 0.978) passing through the origin (data not shown). This result shows that over the time scale of our experiments, the acetone concentration in exhaled air is sufficiently constant. Therefore, it was measured simultaneously with the flavour molecules and used to allow for changing air flow rate in the following way.

The average flavour concentration in the ith exhalation is:

$$[Flavour]_i = \frac{j_{\text{Flavour}}}{V_i}\int_i I_{\text{Flavour}}\mathrm{d}t \qquad (1a)$$

Here V is the volume of expired air and j is the ratio between the amount of flavour molecules and the signal intensity (I). The integral is over one breath peak, so rewriting in terms of the peak area, S_i, gives:

$$[Flavour]_i = \frac{j_{\text{Flavour}}}{V_i}S_{i,\,\text{Flavour}} \qquad (1b)$$

Using this expression for acetone and rearranging gives the volume exhaled:

$$V_i = \frac{j_{\text{Acetone}} \cdot S_{\text{i, acetone}}}{[Acetone]} \qquad (2)$$

Substituting (2) into (1b) gives:

$$[Flavour]_i = [Acetone]\frac{j_{\text{Flavour}}}{j_{\text{Acetone}}}\frac{S_{i,\,\text{Flavour}}}{S_{i,\,\text{Acetone}}} = J \cdot \frac{S_{i,\,\text{Flavour}}}{S_{i,\,\text{Acetone}}} \qquad (3)$$

J is constant for each flavour molecule, subject and experiment. Equation (3) shows that the average concentration of flavour in each breath peak is directly proportional to the ratio between the areas of the flavour and acetone peaks. However, the absolute flavour concentration cannot be determined, because the acetone concentration is unknown. Nevertheless, the shape of the kinetics of flavour release can be compared. To eliminate the effect of air flow rate, all the peak areas are re-scaled relative to the area of the largest acetone peak. Figure 3 shows a typical result of this transformation for menthol (Figure 3a,c) and acetone (Figure 3b,d).

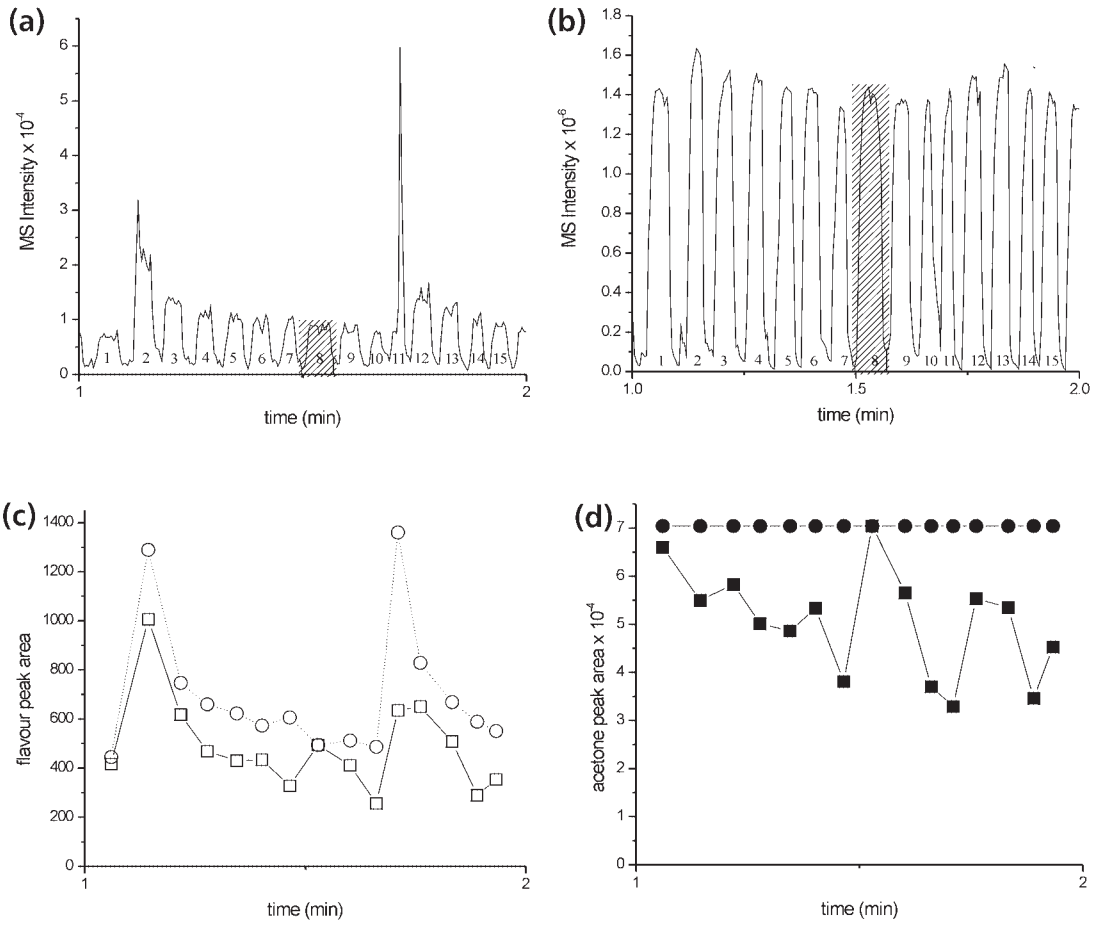

Figure 3 **(a)** Release of menthol during breathing and swallowing. **(b)** Corresponding acetone signal. The reference peak is shaded. **(c)** Menthol peak areas before (open squares) and after (open circles) correction. **(d)** Acetone peak areas before (solid squares) and after (solid circles) correction.

Figure 3a shows that the subject swallowed twice during the experiment (peaks 2 and 11). Figure 3c shows that the raw data for the peak areas (squares) do not decrease regularly. However, the corrected peak areas (circles) are much more regular. This regularity is hidden in the raw data. For the rest of this article, flavour peak areas for each experiment are normalised relative to the largest acetone peak in the experiment.

Before describing the modelling, we want to re-emphasize the importance of using this procedure. In the raw data, peak area for each breath is proportional to the product of exhaled volume and flavour concentration. Data in this form cannot be interpreted in terms of flavour concentration. After normalization, the peak area is proportional to the average concentration (or amount) of flavour released. Using the internal standard removes the ambiguity in interpretation of the data. For instance, in Figure 3c, the raw data after each swallow show a rise in the peak area (sixth breath after the first swallow and fourth breath after the second). The corrected data show that these increases are artefacts, caused by variation in breath volume.

A large set of experimental data (following protocol 2) was obtained from nine subjects drinking aqueous solutions of eight flavour molecules with a wide range of volatilities (see Table 1). The raw data were first treated as described above to average over breath peaks and correct for the effects of air flow rate. Figure 4 shows a typical result, with the area of the breath peaks on a logarithmic scale.

In general, we find that after the first breath, the points fall onto two straight lines, with the first steeper than the second. The first point always falls above the initial steeper line. Following Land (1994) and Buettner *et al.* (2002), we argue that the exhalation that immediately follows swallowing is intrinsically different from all the others. It contains air that is richer in aroma compounds, because it has been in contact with food for longer, in the mouth. For this reason, we do not try to model the first breath after swallowing. The two mathematical models that we now describe explain the origins of the two regimes giving different straight lines. Model I explains the initial steep slope observed just after swallowing. Model II explains the lower slope observed longer after swallowing.

Table 1 Comparison of *in vivo* and *in vitro* partition coefficients of flavour compounds

Flavour molecule	No. of experiments	K_{AS} calculated from equation (7)/10^{-3} (%)	K_{AW} at 25°C/10^{-3}
Dimethyl pyrazine	2	0.58 ± 20	0.07
Ethanol	4	0.48 ± 40	0.6
Menthol	55	1.1 ± 20	1.05
Ethyl acetate	4	1.8 ± 10	3.9
Octanone	4	1.1 ± 15	7.5
Anethole	7	1.0 ± 80	10.5
Citral	7	1.6 ± 40	15.4
Iso-amyl acetate	9	2.5 ± 50	40.0

Model I: equilibrium batch extraction

Surprisingly, the simplest possible model for mass transfer in the throat gives a good description of our data. We assume that the air from each breath has time to equilibrate with the liquid remaining in the throat after swallowing. In other words, we assume that flavour release is due to equilibrium batch extraction. Time is absent, as the system is assumed to be at equilibrium. The same model has been used *in vitro* to measure the partition coefficients of volatile organic compounds (Mackay *et al.*, 1979; Nielsen *et al.*, 1994; Chaintreau *et al.*, 1995). We explain this method in detail, as it is applied in exactly the same way to our *in vivo* data. A syringe is partially filled with a known volume, V_{Water}, of flavoured aqueous solution containing N_{Water} moles of flavour compound. The rest of the syringe is filled with a volume V_{Air} of clean air. Once air–water equilibrium has been reached, the air is pushed out of the syringe and the number of flavour molecules in it, N_{Air}, is determined. The syringe is then refilled with clean air and the whole process is repeated n times. The amount of flavour in the nth batch of expelled air can be calculated using:

$$\begin{cases} (N_{Air})_n = \dfrac{V_{Air}K_{AW}}{V_{Air}K_{AW} + V_{Water}}(N_{Water})_{n-1} \\ (N_{Water})_n = (N_{Water})_{n-1} - (N_{Air})_n \end{cases} \quad (4)$$

K_{AW} is the air–water partition coefficient of the flavour molecule. These equations can be used to calculate N_{Air} as a

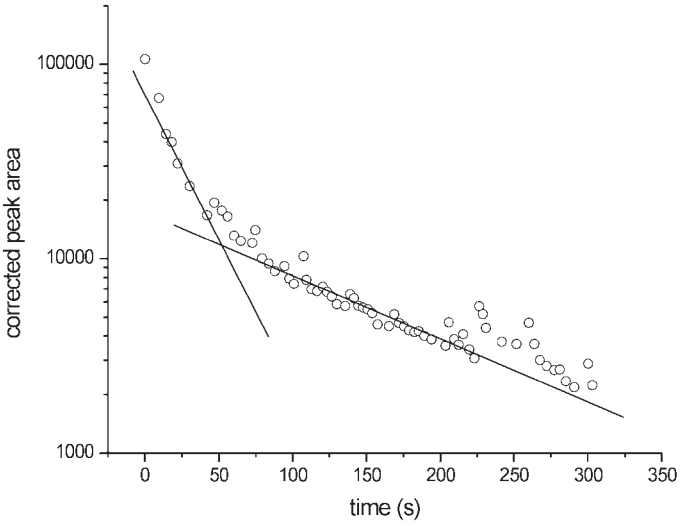

Figure 4 Flavour release after a single swallow of 8 ml of flavoured solution containing 40 p.p.m. of menthol. Lines indicate the two regimes.

function of the initial number of flavour molecules, $(N_{Water})_0$, using:

$$(N_{Air})_n = \frac{V_{Air}K_{AW}}{V_{Air}K_{AW} + V_{Water}}(N_{Water})_0\left(\frac{V_{Water}}{V_{Air}K_{AW} + V_{Water}}\right)^{n-1} \quad (5)$$

Taking logarithms this becomes:

$$\log((N_{Air})_n) = \log\left(\frac{V_{Water}}{V_{Air}K_{AW} + V_{Water}}\right)(n-1) + \log\left(\frac{V_{Air}K_{AW}}{V_{Air}K_{AW} + V_{Water}}(N_{Water})_0\right) \quad (6)$$

This equation has the form $y = px + q$, with p and q constants, so the logarithm of the number of molecules present in a batch of air is proportional to the batch number. Plotting the left-hand side of this equation against the batch number gives a straight line whose slope, p, depends on the partition coefficient, K_{AW}, but is independent of the initial amount of flavour. Rearranging the expression for the slope, we obtain:

$$K_{AW} = \frac{V_{Water}}{V_{Air}}\left(\frac{1 - \exp(p)}{\exp(p)}\right) \quad (7)$$

The key advantage of the method is that partition coefficients can be determined without absolute concentration measurements. Only the ratio of the volume of liquid to the volume of air is needed to calculate the partition coefficient from the slope. By analogy, flavour release data from *in vivo* experiments can be used to obtain an apparent partition coefficient, without needing the absolute flavour concentration in the breath.

We assume that the volume ratio of saliva in the throat to air in the upper respiratory tract is 0.008 (i.e. 100 ml of air for 0.8 ml of saliva in the throat). We justify this value later. This ratio is used in equation (7) to calculate an apparent *in vivo* air–saliva partition coefficient (K_{AS}) from the experimental data. This method of analysis was applied to all the data measured above. Table 1 summarizes the results and compares them with literature values for the volatility (K_{AW}), interpolated to 25°C (J.-Y. de Saint Laumer, private communication). The molecules are listed in order of increasing volatility.

Note that the coefficients of variation tend to be larger for high volatilities. These data are plotted in Figure 5. A solid line indicates the result if the *in vivo* and *in vitro* volatilities were equal.

The most striking observation is that the apparent *in vivo* volatilities all fall within an extremely narrow range: they only vary by a factor of five, whereas the *in vitro* volatilities vary by a factor of >500. Choosing a different air/liquid volume ratio would shift the *in vivo* values vertically, but would not change the slope. Despite the greatly reduced

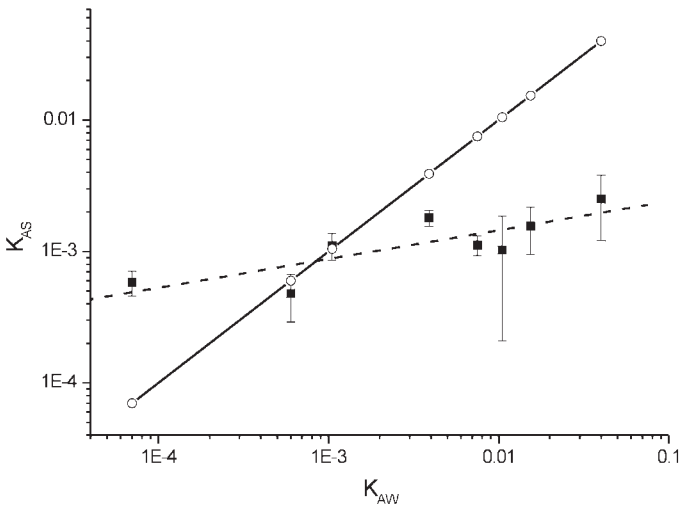

Figure 5 Comparison between K_{AS} measured *in vivo* and literature values of K_{AW} *in vitro*. The solid line is the result expected if $K_{AS} = K_{AW}$. From left to right: dimethyl pyrazine, ethanol, menthol, ethyl acetate, octanone, anethole, citral and iso-amyl acetate.

range, K_{AS} is still roughly proportional to K_{AW}. In fact, it is almost exactly proportional to $(K_{AW})^{1/5}$. This formula is extremely useful for predicting the apparent *in vivo* volatilities of flavour molecules.

When mass transfer between saliva and air is fast, the flavour molecule will be in apparent equilibrium between the two phases and the slope p (and hence K_{AS}) will not depend on the breathing frequency. In this case model I will be applicable. On the other hand, if mass transfer is slow, the system will not be in apparent equilibrium and the slope (and hence K_{AS}) will depend on the breathing frequency.

To test the effect of breathing frequency, two subjects were instructed to breathe with fixed frequency (protocol 3). Experimentally we find that the assumption of equilibrium *in vivo* is reasonable for menthol, ethanol, octanone, ethyl acetate and citral. For anethole and iso-amyl acetate the apparent partition coefficient depends on the breathing frequency, so not even apparent equilibrium is reached. Figure 6 shows the experimentally measured effects of breathing frequency for anethole, which shows breathing frequency dependence, and menthol, which does not.

For breathing frequencies of 2 and 10/min, menthol gives comparable results, whereas the release of anethole depends strongly on breathing rate.

This first model describes the initial slope that begins with the second breath after swallowing. Also, it is very useful for determining the apparent *in vivo* partition coefficient of a flavour molecule, which controls its release after swallowing. However, Figure 4 showed that this simple model only applies for a few breaths after swallowing a liquid. To explain the slower flavour release that occurs longer after swallowing a more elaborate model is needed.

Model II: non-equilibrium and absorption

Model I only applies to the first few breaths after swallowing. Figure 4 showed that after this, the slope decreases continuously and then reaches another regime with a different, constant slope. This can only mean that, after a few breaths, flavour molecules lining the throat move into an environment where they are released more slowly. This environment can only be the throat lining, or mucosa as suggested elsewhere (Buettner *et al.*, 2002). If the flavour molecules were insoluble in the mucosa, then model I would always apply and the logarithm of the flavour peak area would be linear with the breath number throughout the experiment.

Model II includes a layer of mucosa underneath the layer of saliva, so we now have three layers: air, saliva and mucosa. However, just adding another layer to model I is insufficient for two slopes to be observed. Two conditions must be fulfilled: (i) the affinity of flavour molecules must be higher for the mucosa than for air, that is $K_{SM} > K_{AS}$ and (ii) the rate of mass transfer from saliva to air must be much faster than from saliva to mucosa. These two conditions are necessary and sufficient to observe two distinct slopes, with the initial slope being steeper.

Under these conditions, at short times flavour will be released rapidly from the saliva layer into the air. It will also be transferred slowly into the mucosa, but at this point, the transfer is so slow that its effect is not apparent. As time goes on, the loss of flavour to the mucosa becomes large enough to affect the transfer from saliva to the air, which starts to slow, so the slope decreases. Next, the concentration in the mucosa increases to a point where it is in equilibrium with the decreasing concentration in the saliva. This is its maximum concentration. After the next breath, the concentration in the saliva falls below that required to transfer from saliva to mucosa and the process reverses. Finally, the second linear regime is reached where flavour release is limited by transfer out of the mucosa.

Model II abandons the assumption of equilibrium—time is included. Mass transfer between saliva/air and saliva/mucosa are treated as continuous in time and coupled.

Following Hills and Harrison (1995), we choose to model mass transfer using the two-film model. This assumes that both phases are perfectly mixed, so flavour concentrations are equal throughout each phase, except at a very thin region next to each side of the interface. The theoretical expression for the rate of concentration flow through the interface per unit area per unit time (the flux) is given by:

$$f = k(c_{\mathrm{Air}} - K_{\mathrm{AS}} \cdot c_{\mathrm{Saliva}}) \tag{8}$$

Here, k is the overall mass transfer coefficient. This equation shows that mass transfer is driven by the difference between: (i) the actual concentration in one phase and (ii) the concentration that it would have at equilibrium with the actual concentration in the other phase. Note that this expression uses concentration differences in the air. A slightly different expression, but the same flux, would be found if the concentrations in saliva were chosen (see, for instance, Cussler, 1997). To emphasize this point, k should really be called 'the overall air-side mass transfer coefficient'.

We now write the mass balance for each environment, leading to a system of three differential equations:

$$\begin{cases} -\dfrac{\mathrm{d}n_A}{\mathrm{d}t} = \dfrac{k_{SA}S_{SA}}{V_A}n_A - \dfrac{K_{AS}k_{SA}S_{SA}}{V_AK_{AS}+V_S}n_S \\ -\dfrac{\mathrm{d}n_S}{\mathrm{d}t} = \left(\dfrac{K_{AS}k_{SA}S_{SA}}{V_AK_{AS}+V_S} + \dfrac{K_{MS}k_{SM}S_{SM}}{V_MK_{MS}+V_S}\right)n_S - \dfrac{k_{SA}S_{SA}}{V_A}n_A - \dfrac{k_{SM}S_{SM}}{V_M}n_M \\ -\dfrac{\mathrm{d}n_M}{\mathrm{d}t} = \dfrac{k_{SM}S_{SM}}{V_M}n_M - \dfrac{K_{MS}k_{SM}S_{SM}}{V_MK_{MS}+V_S}n_S \end{cases} \tag{9}$$

This system of first-order differential equations can be solved analytically. The solution of each is the sum of three exponentials:

$$\begin{cases} n_A(t) = \displaystyle\sum_{i=1}^{3} \alpha_i Q_i \exp(-\lambda_i t) \\ n_S(t) = \displaystyle\sum_{i=1}^{3} \sigma_i Q_i \exp(-\lambda_i t) \\ n_M(t) = \displaystyle\sum_{i=1}^{3} \mu_i Q_i \exp(-\lambda_i t) \end{cases} \tag{10}$$

where λ_i, α_i, σ_i and μ_i depend on: (i) the mass transfer coefficients (k_{SA} and k_{SM}), (ii) the phase volumes (V_A, V_S and V_M), (iii) the interfacial areas (S_{SA} and S_{SM}) and (iv) the partition coefficients (K_{AS} and K_{MS}). Q_i also depends on the initial quantities [$n_A(0)$, $n_S(0)$ and $n_M(0)$]. Of these 12 parameters, only the mass transfer coefficients and partition coefficients are not fixed by the anatomy, which decreases the number of free parameters to four. In addition, model I gives a good approximation to the apparent K_{AS}, so only three parameters are free.

We now make some reasonable approximations for the variables in the model. The total volume of the upper respiratory tract of a 75 kg human is ~100 cm^3 (Ménache *et al.*, 1997). Then 8 cm^3 of flavoured solution was put into the mouth. We assume that 10% of the solution mixed with saliva covers the throat lining after swallowing. Therefore, 0.8 cm^3 covers the inner surface of a cylinder delimited by the soft palate at the top and the epiglottis at the bottom. The length of the cylinder is estimated as 3.5 cm. The diameter of the throat is taken as 3 cm. These assumptions give the thickness of the saliva coating the throat as 0.25 mm and the contact surfaces for mucosa/saliva and saliva/air as 33 cm^2. At this point, the only remaining adjustable parameters are the two mass transfer coefficients and the apparent saliva-mucosa partition coefficient. Following the careful

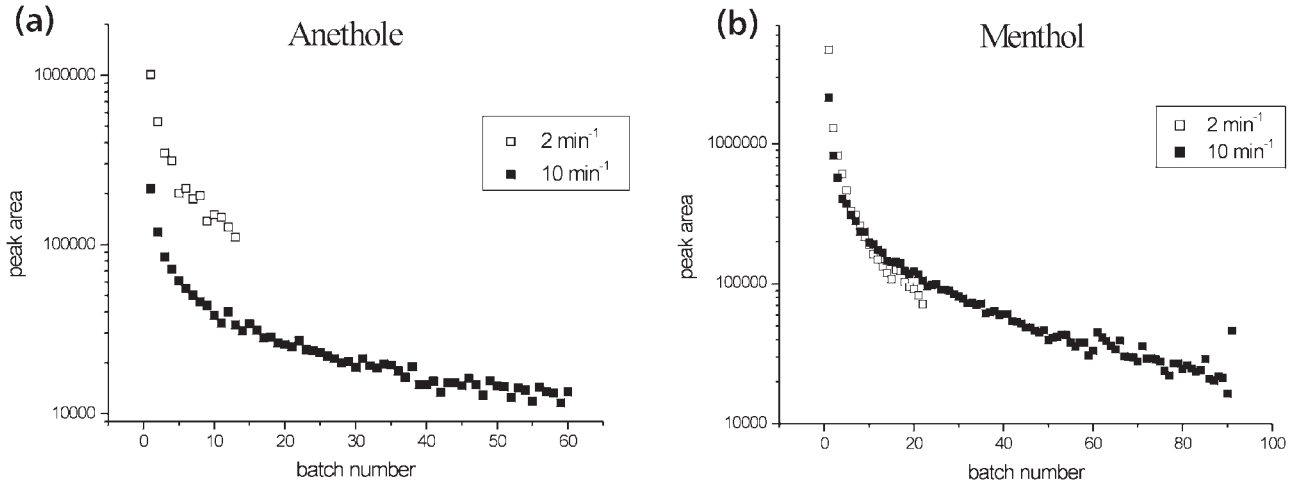

Figure 6 Measured release of anethole **(a)** and menthol **(b)** as a function of breath number, for breathing frequencies of 2 and 10/min.

study of release from water by Marin *et al.* (2000), we set the mass transfer coefficient for air–saliva (k_{SA}) to 3 cm/s. Finally, the presence of two slopes, with the first steeper than the second, implies that flavour in saliva is preferentially partitioned into the mucosa rather than air, i.e. $K_{MS} > K_{AS}$. If this were not true, the second slope would not exist.

This model is continuous in time. However, it retains the idea of batch extraction, as all the air in each breath is assumed to arrive instantly in the throat at the beginning of each exhalation and to disappear instantly at the end of each exhalation. Time and the concentration of flavour molecules in the air are both reset to zero at the start of each exhalation, when clean air arrives in the throat. At the start of each breath, the numbers of molecules in saliva and mucosa are assumed to be equal to those at the end of the previous breath.

We can now calculate the concentrations of flavour in air, saliva and mucosa. Figure 7 shows some typical results.

At time zero, all the flavour is in the saliva. At short times it is transferred to both mucosa and air. At this stage, the amount in the mucosa increases, because it can accumulate from breath to breath. After ~1 min, in this case, the slope for the mucosa changes sign and those for saliva and air become parallel. This is the point at which the flavour concentration in the saliva falls below the level required for transfer from saliva to mucosa. Transfer changes direction to go from the mucosa to the saliva. Transfer to the air is now limited by the rate of flavour transfer from the mucosa, so flavour release falls to a new lower rate.

A non-linear least-squares method was used to fit model II to experimental data. Model I showed that the overall shape of a flavour molecule's release depends on its volatility, but not on its initial concentration. However, the amplitude of the signal is proportional to the initial concentration, so an arbitrary vertical shift in log space is needed to adjust the

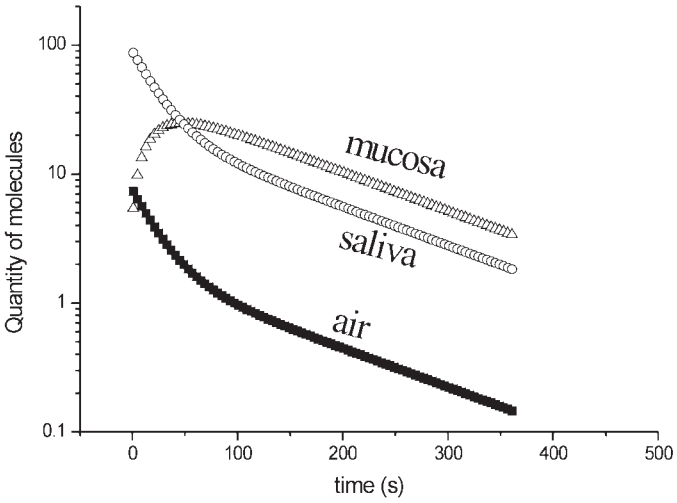

Figure 7 Simulation using model II for the quantity of molecules present in the three media. The initial number of flavour molecules in saliva is arbitrarily set to 100 and no flavour molecules are present initially in the air and in the mucosa. The breathing frequency is constant at 15/min. Parameter values: $k_{SA} = 3$ cm/s, $k_{SM} = 3 \times 10^{-3}$ cm/s, $K_{AS} = 1.3 \times 10^{-3}$ and $K_{MS} = 10^3$.

model to the experimental data. Figure 8 shows the good fit of model II to typical experimental data.

The best fit is obtained with the following parameter values: $k_{SA} = 0.3$ cm/s, $k_{SM} = 1.7\ 10^{-3}$ cm/s and $K_{MS} = 192$. As implied by the existence of two slopes in Figure 4, the mass transfer coefficient for saliva–air is ~200 times larger than that for saliva-mucosa. In addition, the large value of K_{MS} shows that flavour partitioning is in favour of the mucosa.

Effects of varying parameter values in model II

Figure 9 shows how varying each of the three key parameters and the breathing frequency affects the kinetics of

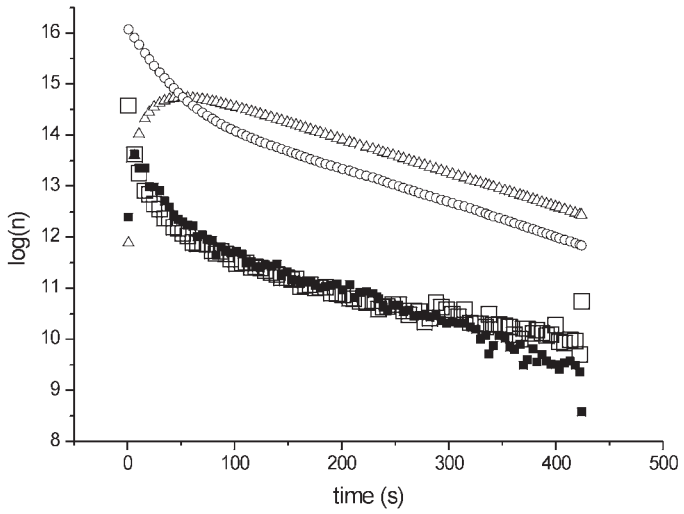

Figure 8 Comparison of experimental data measured in air (open squares) with calculation using model II (solid squares). Calculated quantities in saliva (open circles) and mucosa (open triangles) are also shown. Calculated data have an arbitrary vertical shift for easy comparison of the shapes.

flavour release predicted by model II. Arrows show how the shape of the curve changes as the parameter increases.

Figure 9a shows that small changes in the saliva–air mass transfer coefficient have a large effect on both the initial and final slopes. The initial slope decreases as this mass transfer coefficient increases, whereas the final slope increases. However, both slopes tend towards limiting values as the rate of transfer increases.

In contrast, Figure 9b shows that changing the saliva-mucosa partition coefficient has a smaller effect on the kinetics of flavour release. The final slope is more affected than the initial slope.

Figure 9c shows that varying the saliva–mucosa mass transfer coefficient has a significant effect on the point of inflection separating the two slopes. The lower the saliva–mucosa mass transfer coefficient, the later the point of inflexion occurs. Intuitively, slowing the rate of transfer increases the time needed to reach saliva-mucosa equilibrium.

Figure 9d shows the effects of changing the breathing frequency. Under our chosen conditions, model II agrees with the observation illustrated in Figure 6b: changes in breathing frequency have no effect on the initial slope under normal human breathing frequencies. Only unrealistically low breathing frequencies influence the initial flavour release. At normal breathing frequencies, the flavour does not have time to penetrate sufficiently into the mucosa.

Discussion

The models formulated here for flavour release during drinking combine realistic physiological assumptions with the simplest possible models for the liquid/air mass transfer. This is a deliberate choice: we want to gain insight from approximate models with a few parameters before progressing to more detailed models. The realistic physiology distinguishes our work from that of Harrison (1998, 2000). In our opinion, his first model (Harrison, 1998) is fatally flawed by the assumption that air is continuously flowing from the lungs through the mouth to the nose. His second model, for release from chewing gum (Harrison, 2000), assumes that flavour-rich air from the mouth is pumped into the exhaled air at each chew. This is a better approximation to reality, for chewing gum. However, the assumption is clearly quite unable to explain flavour release during drinking. On the other hand, Land (1994) and Buettner *et al.* (2002) deduce flavour concentrations in exhaled air directly from physiological measurements. They assume that no flavour can reach the nose if the soft palate is closed. Our results show that this is not true. In fact, Linforth and Taylor (2000) have shown sequences of peaks similar to those in Figure 2; see their Figure 1. However, they do not try to explain the whole sequence after swallowing. They define the ratio of the first peak height to the second peak height as the 'persistence' and relate this value directly to the molecular properties of volatiles, using chemometrics.

The models for mass transfer are clearly unrealistic: model I assumes equilibrium. Both models assume instant, perfect mixing in all phases. Mass transfer is lumped over each exhalation. They are far from the sophistication of Keyhani et al.'s (1997) model for odorant mass transfer in the nose, during sniffing. The simplicity of our models means that, for instance, we have nothing to say about the change in flavour concentration during a breath. Nor can we address the question of how changes in the concentration of aroma molecules over the nasal epithelium might affect perception, as discussed by Keyhani *et al.* (1997). Nevertheless, we think that they give insight into the basic processes by which aroma molecules are transferred to exhaled air during drinking. The models make non-trivial, testable predictions that we have shown are compatible with a sizeable data set.

Unexpectedly, model I shows that apparent air–saliva partition coefficients fall within a very narrow range. The decreasing slope at long times, described by model II, can only be interpreted by assuming that the air–mucus partition coefficient is significantly lower than that for air–saliva. Keyhani *et al.* (1997) assume that air–mucus partition coefficients are equal to those for air–water, stating that there are no experimental measurements for air–mucus partition. Our results are incompatible with this assumption.

Summary and conclusions

The kinetics of flavour release during drinking vary hugely between subjects. These differences are mainly due to variations in the pattern of swallowing and breathing. Interpretation of 'nose space' data in terms of flavour concentrations can only be done after correcting for the effect of air flow rate. Exhaled acetone can be used to do this. We have shown that during drinking, only a small amount of aroma-rich air

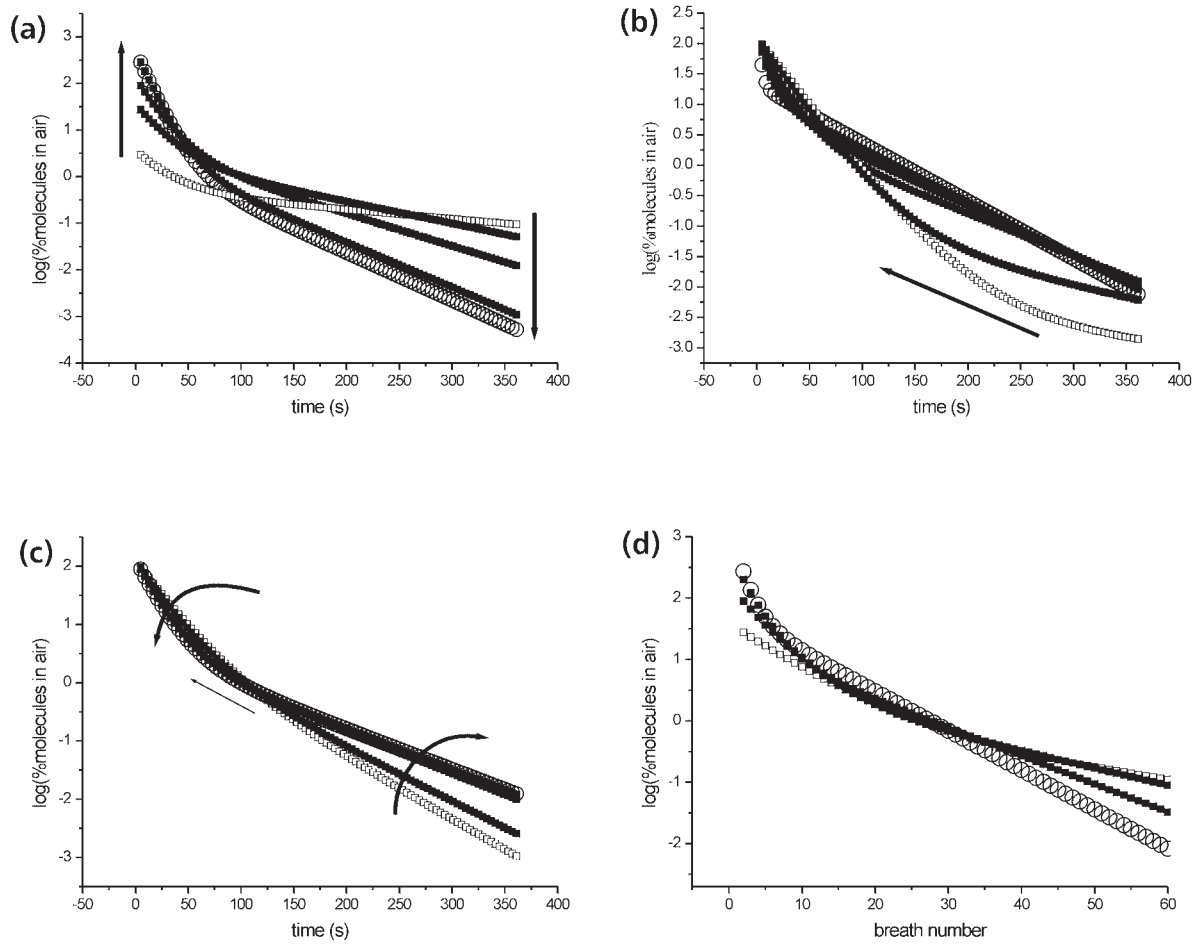

Figure 9 Effect of varying key parameters in model II on the calculated kinetics of flavour release. Base case uses $K_{MS} = 10^3$, $k_{SA} = 0.6$ cm/s, $k_{SM} = 3 \times 10^{-3}$ cm/s and breathing frequency = 15/min. **(a)** Vary k_{SA}: 0.1 (open squares), 0.3, 0.6, 2 and 10 cm/s (open circles). **(b)** Vary K_{MS}: 0.05 (open squares), 0.1, 1, 10 and 1000 (open circles). **(c)** Vary k_{SM}: 5×10^{-4} (open squares), 10^{-3}, 3×10^{-3}, 5×10^{-3}, 7×10^{-3}, 10^{-2} and 3×10^{-2} cm/s (open circles). **(d)** Vary the breathing frequency: for values 2 (open squares), 4, 8 and 16/min (open circles).

passes direct from mouth to nose, just after swallowing. The rest of the time, the aroma signal in the nose is extracted from liquid in the throat by exhaled air. Flavour release after a swallow during drinking falls into three regimes: (i) the first breath, which is abnormally large, contains air from the mouth; (ii) the next few breaths where release can be assumed to be from a liquid film coating the throat; and (iii) the rest of the breaths for which interaction with the mucosa must be considered.

Two simple models for mass transfer in the throat correctly encapsulate the trends observed experimentally when the data are treated breath by breath. More sophisticated models will be needed to understand the fine structure of flavour release during each breath.

Our overall aim was to obtain physico-chemical parameters from real time flavour release data that are independent of the panellist's behaviour. We feel that we have succeeded in this task, perhaps surprisingly well, considering the simplicity of the models.

Acknowledgements

Our thanks to Tony Blake, Bénedicte Ribot and Jérôme Barra for their help and advice.

References

Bosma, J.F. (1980) *Physiology of the mouth, pharynx, and oesophagus. Physiology of the mouth*. In Paparella, M.M. and Shumrick, D.A. (eds), Otolaryngology. W.B. Saunders, Philadelphia, PA, pp. 319–331.

Buettner, A., Beer, A., Hannig, C. and **Settles, M.** (2001) *Observation of the swallowing process by application of videofluoroscopy and real time magnetic resonance imaging—consequences for retronasal aroma stimulation*. Chem. Senses, 26, 1211–1219.

Buettner, A., Beer, A., Hannig, C., Settles, M. and **Schieberle, P.** (2002) *Physiological and analytical studies on flavor perception dynamics as induced by the eating and swallowing process*. Food Qual. Pref., 13, 497–504.

Cussler, E.L. (1997) Diffusion Mass Transfer in Fluid Systems. Cambridge University Press, Cambridge.

Chaintreau, A., Grade, A. and **Munoz-Box, R.** (1995) *Determination of partition coefficients and quantification of headspace volatile compounds*. Anal. Chem., 67, 3300–3304.

Dodds, W.J., Stewart, E.T. and **Logemann, J.A.** (1990a) *Physiology and radiology of the normal oral and pharyngeal phases of swallowing*. Am. J. Roentgenol., 154, 953–963.

Dodds, W.J., Logemann, J.A. and **Stewart, E.T.** (1990b) *Radiologic assessment of abnormal oral and pharyngeal phases of swallowing*. Am. J. Roentgenol., 154, 965–974.

Firmin, H., Reilly, S. and **Fourcin, A.** (1997) *Non-invasive monitoring of reflexive swallowing*. Speech, Hearing Lang., 10, 171–184.

Harrison, M. (1998) *Effect of breathing and saliva flow on flavor release from liquid foods*. J. Agric. Food Chem., 46, 2727–2735.

Harrison, M. (2000) Mathematical Models of Release and Transport of Flavors from Foods in the Mouth to the Olfactory Epithelium, ACS Symposium Series 763 (Flavour Release), pp. 179–191.

Hills, B.P. and **Harrison, M.** (1995) *Two-film theory of flavour release from solids.* Int. J. Food Sci. Technol., 30, 425–436.

Hodgson, M., Linforth, R.S.T. and **Taylor, A.J.** (2003) *Simultaneous real time measurements of mastication, swallowing, nasal airflow and aroma release*. J. Agric. Food Chem., 51, 5052–5057.

Keyhani, K., Scherer, P.W. and **Mozell, M.W.** (1997) *A numerical model of nasal odorant transport for the analysis of human olfaction*. J. Theor. Biol., 186, 279–301.

Land, D.G. (1994) Perspectives on the Effects of Interactions on Flavor Perception: An Overview. ACS Symposium Series 633, pp. 2–11.

Linforth, R.S.T. and **Taylor, A.J.** (1998) *Apparatus and methods for the analysis of trace constituents of gases.* European patent EP 0819 937 A2.

Linforth, R.S.T. and **Taylor, A.J.** (2000) *Persistence of volatile compounds in the breath after their consumption in aqueous solutions*. J. Agric. Food Chem., 48, 5419–5423.

Mackay, D., Shiu, W.Y. and **Sutherland, R.P.** (1979) *Determination of air–water Henry's law constants for hydrophobic pollutants*. Environ. Sci. Technol., 13, 333–337.

Marin, M., Baek, I. and **Taylor, A.J.** (2000) Flavor Release as a Unit Operation: A Mass Transfer Approach Based on a Dynamic Headspace Dilution Method. ACS Symposium Series 763, pp. 153–165.

Ménache, M.G., Hanna, L.M., Gross, E.A., Lou, S.-R., Zinreich, S.J., Leopold, D.A., Jarabek, A.M. and **Miller, F.J.** (1997) *Upper respiratory tract surface areas and volumes of laboratory animals and humans: considerations for dosimetry models.* J. Toxicol. Environ. Health, 50, 475–506.

Nielsen, F., Olsen, E. and **Fredenslund, A.** (1994) *Henry's law constants and infinite dilution activity coefficients for volatile organic compounds in water by a validated batch air stripping method*. Environ. Sci. Technol., 28, 2133–2138.

Taylor, A.J. (2002) *Release and transport of flavours* in vivo*: physicochemical, physiological, and perceptual considerations*. Compr. Rev. Food Sci. Food Safety, 1, 45–57.

Taylor, A.J. and **Linforth, R.S.T.** (2000) Techniques for Measuring Volatile Release *In-vivo* during Consumption of Food. ACS Symposium Series 763, pp. 8–21.

Taylor, A.J., Linforth, R.S.T., Harvey, B.A. and **Blake, A.** (2000) *Atmospheric pressure chemical ionisation mass spectrometry for* in vivo *analysis of volatile flavour release*. Food Chem., 71, 327–338.

Accepted January 28, 2004